Metadata of the chapter that will be visualized in SpringerLink

Book Title	Advances in Self-Organizing Maps and Learning Vector Quantization	
Series Title		
Chapter Title	The Effect of SOM Size and Similarity Measure on Identification of Functional and Anatomical Regions in fMRI Data	
Copyright Year	2016	
Copyright HolderName	Springer International Publishing Switzerland	
Corresponding Author	Family Name	**O'Driscoll**
	Particle	
	Given Name	**Patrick**
	Prefix	
	Suffix	
	Division	
	Organization	Applied Physics Program, Rice University
	Address	Houston, TX, USA
	Email	patrick.odriscoll@rice.edu
		po2@rice.edu
Author	Family Name	**Merényi**
	Particle	
	Given Name	**Erzsébet**
	Prefix	
	Suffix	
	Division	
	Organization	Department of Statistics and Department of Electrical & Computer Engineering, Rice University
	Address	Houston, TX, USA
	Email	erzsebet@rice.edu
Author	Family Name	**Karmonik**
	Particle	
	Given Name	**Christof**
	Prefix	
	Suffix	
	Division	Department of Neurosurgery, Houston Methodist Neurological Institute
	Organization	Houston Methodist Research Institute
	Address	Houston, TX, USA
	Email	CKarmonik@houstonmethodist.org
Author	Family Name	**Grossman**
	Particle	
	Given Name	**Robert**
	Prefix	
	Suffix	
	Division	

Organization	Weill Medical College of Cornell University
Address	New York, NY, USA
Email	RGrossman@houstonmethodist.org

Abstract	We demonstrate the advantage of larger SOMs than those typically used in the literature for clustering functional magnetic resonance images (fMRI). We also show the advantage of a connectivity similarity measure over distance measures for cluster discovery and extraction. We illustrate these points through maps generated from a multiple-subject investigation of the genesis of willed movement, where clusters of the fMRI time-courses signify functional (or anatomical) regions, and where accurate delineation of many clusters is critical for tracking the relationships of neural activities across space and time. While we do not provide an automated optimization of the SOM size it is clear that for this study increasing it up to 40×40 facilitates clearer discovery of more relevant clusters than from a 10×10 SOM (a size frequently used in the literature), and further increase has no benefits in our case despite using large data sets (all data from whole-brain scans). We offer insight through data characteristics and some objective justification.

Keywords (separated by '-')	Conscience self-organizing map - CONNvis - Cluster extraction - Functional magnetic resonance imaging - Willed movement - Data-driven model

The Effect of SOM Size and Similarity Measure on Identification of Functional and Anatomical Regions in fMRI Data

Patrick O'Driscoll, Erzsébet Merényi, Christof Karmonik and Robert Grossman

Abstract We demonstrate the advantage of larger SOMs than those typically used in the literature for clustering functional magnetic resonance images (fMRI). We also show the advantage of a connectivity similarity measure over distance measures for cluster discovery and extraction. We illustrate these points through maps generated from a multiple-subject investigation of the genesis of willed movement, where clusters of the fMRI time-courses signify functional (or anatomical) regions, and where accurate delineation of many clusters is critical for tracking the relationships of neural activities across space and time. While we do not provide an automated optimization of the SOM size it is clear that for this study increasing it up to 40 × 40 facilitates clearer discovery of more relevant clusters than from a 10 × 10 SOM (a size frequently used in the literature), and further increase has no benefits in our case despite using large data sets (all data from whole-brain scans). We offer insight through data characteristics and some objective justification.

This work was partially supported by the Program for Mind and Brain, Department of Neurosurgery, Houston Methodist Hospital. Figures are in color, request a color copy by email: patrick.odriscoll@rice.edu, erzsebet@rice.edu

P. O'Driscoll (✉)
Applied Physics Program, Rice University, Houston, TX, USA
e-mail: patrick.odriscoll@rice.edu; po2@rice.edu

E. Merényi
Department of Statistics and Department of Electrical & Computer Engineering, Rice University, Houston, TX, USA
e-mail: erzsebet@rice.edu

C. Karmonik · R. Grossman
Department of Neurosurgery, Houston Methodist Neurological Institute, Houston Methodist Research Institute, Houston, TX, USA
e-mail: CKarmonik@houstonmethodist.org

R. Grossman
e-mail: RGrossman@houstonmethodist.org

C. Karmonik
Weill Medical College of Cornell University, New York, NY, USA

E. Merényi et al. (eds.), *Advances in Self-Organizing Maps and Learning Vector Quantization*, Advances in Intelligent Systems and Computing 428,
DOI 10.1007/978-3-319-28518-4_22

340050_1_En_22_Chapter ☑ TYPESET ☐ DISK ☐ LE ☑ CP Disp.:18/12/2015 Pages: 264 Layout: T1-Standard

Keywords Conscience self-organizing map · CONNvis · Cluster extraction · Functional magnetic resonance imaging · Willed movement · Data-driven model

1 Background and Motivation

In this paper we aim to demonstrate that SOM size significantly influences cluster identification. We also aim to demonstrate the benefits of a connectivity based (rather than distance based) measure for cluster extraction from a converged SOM. To do this we analyze full brain functional magnetic resonance imaging (fMRI) data of humans generating willed movement initiated from a visual stimulus. fMRI is an accepted method to non-invasively infer real-time neural activity from a hemodynamic response known as the blood oxygen level dependence (BOLD) signal. fMRI data comprises time-courses, or time-series, of the BOLD signal at each voxel in a regular three-dimensional grid over a brain volume. Traditionally, a map reflecting neural activity level is constructed by computing the statistical likelihood of each voxel's fit to a given model of the BOLD signal. Activity maps, however, only provide a comparison of the activation strengths of various regions, but do not reveal the functional relationships of the activation patterns (time-courses).

Voxels clustered based on the similarity of their time-courses can be used to identify functional regions of the brain, in a model-free (data-driven) approach. Various techniques including graph based, statistical, and artificial neural network methods have been applied for this purpose. Kohonen SOMs [1] in particular, have been successful in either outperforming other methods or providing deeper insights (e.g., [2–6]). While it is widely known that too small SOMs can be suboptimal for cluster extraction, fMRI studies tend to use small SOMs ranging from 3×3 to 12×12 neurons, often trained only on selected subsets of the available data. Such small SOMs can work for specific goals as in the examples we review below. We will argue, however, that larger SOMs could allow more detailed discoveries or more comprehensive analyses of the whole brain.

Authors of [2–4] use the whole brain (or substantial portion) but constrain their focus to relatively few functional regions. The interest in [2] is to capture 4–5 functional regions from each of the resting and a goal directed state. After experimenting with SOM sizes ranging from 4×4 to 12×12 neurons the authors conclude that a 10×10 SOM suffices for finding the targeted functional regions. A 10×10 SOM is used by [3] to examine the effects of age on autism, by capturing 16 clusters that represent a handful of expected active areas of the rest state and the default mode network (DMN). Similarly, 10–20 clusters are extracted from a 11×11 SOM in [4], delineating expected regions mainly in the motor cortex. Other studies limit the amount (and complexity) of the data by processing only selected parts. Both [5, 6] take the widely used approach of excluding voxels that fall below some activation level. [5] uses unsupervised SOM, [6] uses supervised SOMs to obtain a small number of clusters/classes (3–8) of very small numbers of voxels (few hundred to a few thousands), and evaluate clustering quality or classification accuracy as a function of the number of voxels processed. The SOMs are small (6×4 in [5], undeclared

size in [6] but look no larger than $\sim 10 \times 10$.) [5] concludes that keeping only active voxels with increasing ROI specificity (smaller and smaller sets of voxels) improves results. [6] shows that increasing the ratio of active voxels to inactive ones improves classification, albeit the accuracies are rather low ($\lessapprox 0.5$ for real data). However, neither paper investigates how a larger SOM would facilitate better results by coping with more voxels or providing more resolution for cluster separation. For clustering the SOM, typically ℓ_2-distance based measures are applied although some works use more sophisticated clustering methods than others. Visualization, where used, is most often the plotting of prototype vectors into their SOM grid locations.

In this work we show the benefits of using larger SOMs than those typically found in fMRI literature, and we also show the advantage of using a non-distance-based metric to extract clusters from converged SOMs. We demonstrate these points on *whole brain* fMRI data.

2 Data Collection, Acquisition, and Pre-processing

Here we describe the experiment performed for our data collection, the acquisition parameters and resulting dataset, and the pre-processing of that data.

Experiment A series of ten human faces (five pleasant and five unpleasant) are presented to subjects in a random order, generally with a 50s rest period. Each face is shown for 10s, and judged by the subject to be pleasant or unpleasant. The subject is instructed to squeeze a ball placed in his/her right hand if the face is judged to be unpleasant, until the face goes away. If the subject finds the face pleasant, he/she does nothing. Figure 1 shows part of the experiment with expected BOLD signals, generated in the left motor cortex, as a result of the subject's reaction to unpleasant faces. When the subject sees an unpleasant face, he/she makes a willed movement, thereby generating a series of neural activities that travel through both time and space in the brain. The activity originates in the visual cortex upon perceiving the face, then travels to other parts of the brain, and finally reaches the left sensory-motor cortex when the subject squeezes the ball. We are investigating the spatial and temporal relationships between the areas of the brain that participate in this process. In this paper we concentrate on describing the methods used to extract this information by clustering.

Data Acquisition and Pre-processing The data of six subjects from a larger study under an IRB approved protocol are analyzed. The fMRI data is collected using a Siemens Vario 3 Tesla scanner. Each subject sees each face for 10s. The duration of the rest period is generally 50s, long enough to allow the expected BOLD signal to completely subside before the next face presentation. The voxel size ranges between $2.750 \times 2.750 \times 5.000$ mm^3 and $3.594 \times 3.594 \times 5.000$ mm^3, the temporal resolution varies from 1.0 to 1.5s per brain scan across subjects, yielding data cubes of $\sim 64 \times 64 \times 24 \times 460$ (i.e. approx. 100 k time-courses each with approx. 460 samples). Pre-processing follows that in [7], which performed well in our experiments: motion correction, high- and low-pass filtering (which removes signal outside the

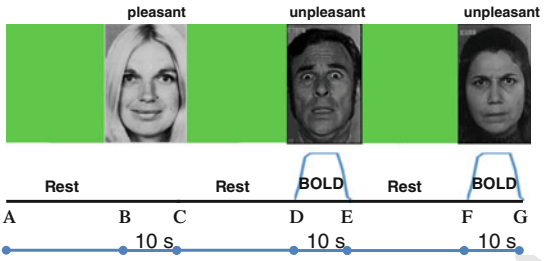

Fig. 1 Sample experiment consisting of showing three faces (one pleasant, and two unpleasant). Time windows A to B, C to D, and E to F are rest periods, B to C is a pleasant face presentation, and D to E and F to G are unpleasant face presentations. The expected BOLD signal (in the left motor cortex) is shown for the two unpleasant face presentations, our windows of interest

0.008–100.0 Hz frequency range), and each time-course is scaled by its ℓ_2-norm. Areas outside the brain are masked (excluded) from processing. All these steps are carried out using AFNI [8], an open source data visualization and processing software. To concentrate on relevant information in the time-courses, the windows of interests—such as the windows of face showing—may be extracted and concatenated to form the input vectors for clustering. We follow another approach using a single window. Since data from the first unpleasant face presentation is most likely to be free of irrecoverable artifacts in all subjects we use an interval of 36 points (40–50s) encompassing the entire ramp up and down of the BOLD signal generated by this event.

3 Analysis Methods

We use a SOM with conscience learning, or Conscience SOM (CSOM) [9], for maximum entropy (equiprobabilistic) mapping, thus potentially more faithful matching of the *pdf* of the data by the SOM prototypes. Compared to the Kohonen SOM algorithm, this is achieved by the use of a *bias* at winner selection, thereby discouraging frequently winning nodes from winning and encouraging infrequent winners to win more:

$$c(\mathbf{x}) = argmin_i(||\mathbf{x} - \mathbf{w}_i|| - bias_i), i = 1, ..., N \quad (1)$$

Here N is the number of SOM prototypes $\mathbf{w}_i \in R^n$, $\mathbf{x}$ is a point in the data manifold $M \subset R^n$, and c indices the winning prototype $\mathbf{w}_c$. The bias for prototype $\mathbf{w}_i$ is computed as in Eq. (2) where γ is a user-controlled parameter, and F_i is the winning frequency of w_i, updated after each learning step. The weight update rule remains the same as for the KSOM (Eq. 3).

$$bias_i = \gamma(1/N - F_i) \quad (2)$$

$$\mathbf{w}_i(t+1) = \mathbf{w}_i(t) + \alpha(t)h_{c,i}(t)(\mathbf{x} - \mathbf{w}_i(t)) \quad (3)$$

The CSOM neighborhood function $h_{c,i}$ can have a constant small radius r (of 1 or 2) throughout the learning process because the "conscience" ensures the propagation of collaboration among prototypes. We use $r = 1$ or $r = \sqrt{2}$, (updating the 4 or 8 immediate neighbors in diamond-shaped or square neighborhoods, respectively), in a rectangular lattice. This significantly reduces computational cost. The equiprobabilistic mapping property of the CSOM was shown in [9] for 1-dimensional data, and demonstrated for higher-dimensional data in [10, 11].

Cluster Extraction For capturing clusters of fMRI time-courses from converged SOMs we compare the relative merits of two frequently used inexpensive visualizations, mU-matrix [10] and the plot of prototype vectors at their SOM grid locations, with CONNvis [12] (Fig. 2). We note that visualizations such as the U, P, AU*, AP matrices [13] (and references therein) — which are attractive, and effective when used on an emergent SOM. However this requires the number of prototypes to be close to the number of data points which is not practical in our case due to the large data size. Just as importantly, large number of prototypes does not help clustering of our fMRI data, as we will see.

The mU-matrix [10] is a refinement of the classic U-matrix [14]. It represents the Euclidean distance of a prototype to each of its eight lattice neighbors. The distances are visualized as thin gray-scale "fences" between adjacent SOM grid cells (instead of shading each grid cell to the average value of the distances). Dark fence means small distance, bright fence means strong separation and therefore may indicate cluster boundary. The mU-matrix also encodes the mapping density by the brightness of a monochrome cell color (red in Fig. 2a) which is proportional to the number of data points mapped to the cell. An example can be seen in Fig. 2a. We also plot the prototypes at their lattice locations as it is a customary way to show the learned SOM in fMRI studies, and it provides a direct visual assessment of the pattern differences (Fig. 2c).

The CONNvis is a visualization of the CONN similarity measure, which expresses *connectivity* rather than distances. The connectivity, $CONN(i, j)$, of two prototypes w_i, w_j, is the number of times w_i and w_j are selected as a pair of best matching unit (BMU) and second BMU for any data point. $CONN(i, j) > 0$ means that w_i, w_j are Voronoi neighbors in M. The visualization shows the connectivity for every pair of prototypes (black points in Fig. 2b) by a connecting line where the line width is proportional to the (normalized) $CONN$ value. For visualization purposes the line widths are also binned to help the human eye. The binning, described in detail in [12], is non-linear and governed by the data statistics. Discontinuities or weakly connected regions of the manifold emerge where no or very thin connections are drawn. The connections of a prototype to its Voronoi neighbors are ranked by their relative strengths and the ranking is indicated by colors: red line connects to the most important Voronoi neighbor, followed by blue, green, yellow, and gray shades. The ranking expresses local manifold relations and provides finer details for the identification of cluster boundaries. As an additional benefit CONNvis shows topology violations: prototypes connected with line segments longer that one lattice unit violate topology preservation. The line width indicates the severity of the violation. A procedure for

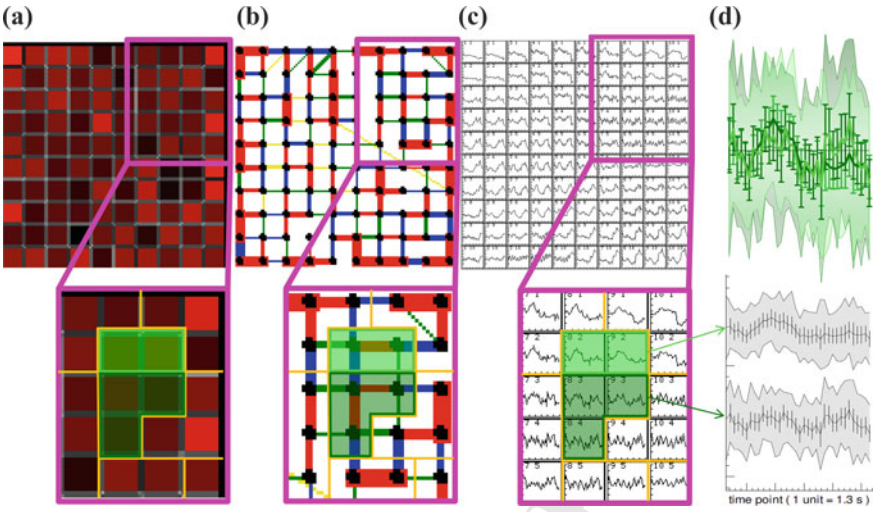

Fig. 2 Example of extracting two clusters belonging to the visual cortex from three different visualizations of a 10 x 10 CSOM. These two clusters are indicated by the *light green* and *dark green* outlines, highlights and lines. **a** mU-matrix, **b** CONNvis, **c** prototypes plotted at their SOM grid cells, and **d** *top*: average time-courses of the two *green* clusters vertically exaggerated and overlain for comparison, with standard deviations (*vertical bars*), and ranges shown; bottom: the same two average time-courses shown separately. Other clusters found in the boxed SOM area (some also related to the visual cortex) are outlined in *orange*. The mU-matrix representation, which expresses clusters well for many other types of data, seems insensitive to the small differences in prototype distances that appear to characterize fMRI data. Owing to the connectivity measure, the CONNvis shows clearer clusters despite their high degree of similarity. The shapes of the prototypes are consistent with the extracted clusters

cluster extraction based on CONNvis is also outlined in [12]. Figure 2 shows an example of extracting two clusters, indicated in green boxes, from a 10×10 CSOM. In Fig. 2b these are defined by groups of prototypes with strong connections to each other (thick red lines) while each group's connection to another group of prototypes is less strong (blue lines). The two clusters highlighted in green primarily make up the visual cortex. Their close relationship is expressed by the strong ranking (blue) of their interconnections in the CONNvis representation. Figure 2c provides evidence for this grouping. Other clusters in this inset are indicated in orange boxes but not discussed here.

Data Post-Processing For the purpose of tracking the generation of the willed movement, we filter the extracted SOM clusters for displays of brain maps showing associations with the visual stimulus and the clenching of the right fist. The filtered clusters are those whose average time-courses correlate relatively strongly with the mean of the cluster identified as the visual cortex. Other clusters are assumed to represent the rest state or other involvement. The correlation threshold, in this case 0.5, is empirically determined and can vary for different data and tasks. Our discussion of the clustering quality as a function of SOM size, however, includes all clusters we delineate, not only the filtered ones.

4 Effects and Evaluation of SOM Size

All clusters extracted from the 10 × 10 SOM in Fig. 2, and from a 40 × 40 SOM (18 and 29, respectively) can be seen in Fig. 3. Filtered clusters mapped back to two selected brain slices are shown in Fig. 4. The quality of the extracted clusters can greatly differ depending on the SOM size. By allocating more prototypes to high-density areas, the 40 × 40 SOM facilitates separation of groups of similar fMRI time-courses with small but consistent differences. This translates to finer spatial resolution and delineation of more, functionally distinct, areas in the brain than from the 10 × 10 SOM. An example can be seen by the comparisons made in Fig. 4. While clusters belonging to the superior frontal and medial frontal gyri (the magenta clusters) are detected from both the 10 × 10 and 40 × 40 SOMs, the 40 × 40 SOM also allows to fully resolve the sensory-motor area (dark red cluster), and the detection of the cerebellum (dark blue cluster). These regions cannot be mapped from the 10 × 10 SOM without including large swaths of other brain areas. The visual cortex is

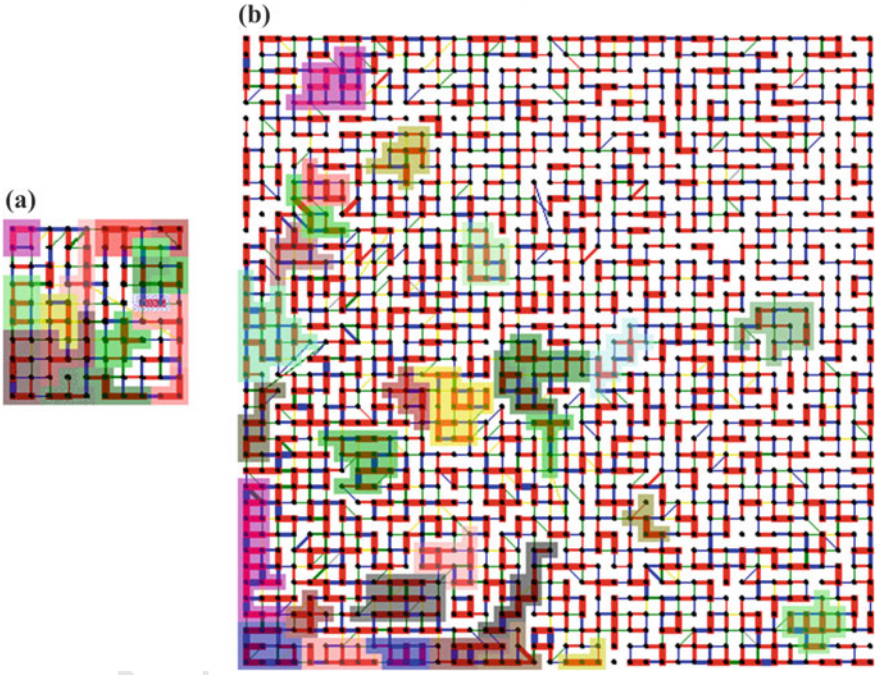

Fig. 3 CONNvis of **a** 10 × 10 and **b** 40 × 40 CSOM, overlain with extracted clusters (colored groups of prototypes). The color coding of clusters belonging to the same functional regions in the brain is as similar as possible in the two SOMs, but cannot be made identical due to more resolved clusters in the 40 × 40 SOM. Unclustered areas of the 40 × 40 SOM contain prototype groups that map to spatially incoherent sets of voxels or unimportant features in the brain (such as spinal fluid). Data: Subject 2

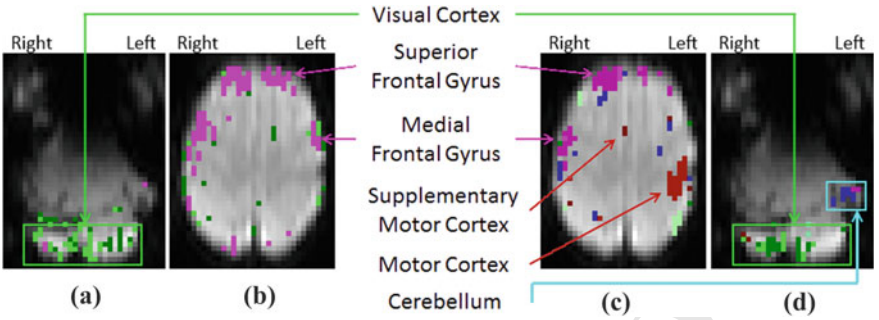

Fig. 4 Comparison of clusters extracted from the 10×10 and 40×40 CSOMs in Fig. 3, filtered and mapped to the brain. The two selected axial slices display clusters associated with the visual, motor, and cognitive functions. **a**, **b**: Clusters identified from the SOM in Fig. 3a. **c**, **d**: Clusters identified from the SOM in Fig. 3b

resolved in both SOMs (Figs. 4a and d). Both these clusterings as well as one from a 20×20 SOM were validated and compared by neuroscientist experts, judging the 40×40 clustering as significantly better than the others.

The advantage of the larger SOM size can also be measured objectively using cluster validity indices. There exist many indices, and some are better suited for high-dimensional data with complex cluster structure than others. We give here measurements by four indices, listed in columns 3–6 of Table 1. Two of them, the classic Davies-Bouldin Index (DBI, [15]), and the newer Pakhira-Bandyopadhyay-Maulik-index (PBM) favors spherical clusters when ℓ_2 distances are used. PBM strongly favors a small number of clusters (penalizes the number of clusters quadratically). Composed density between and within clusters ($CDbw$) rewards clusters with homogeneous density. $CONNindex$ [16] is a recent one developed to address difficulties caused by irregular clusters and complicated cluster structure. We sketch the essence of DBI and $CONNindex$ below. Due to space constraints please see formulae and references for PBM and $CDbw$ in [16].

DBI is defined as the average, over all clusters, of the maximum ratio of the average intra-cluster scatter (standard deviation in this case) to the inter-cluster separation. The inter-cluster separation is the distance between cluster centers. $CONNindex$ relies on the $CONN$ connectivity measure [12]. As defined in [16], $CONNindex = Intra\_Conn \times (1 - Inter\_Conn)$ where $Intra\_Conn$ is the average *intra-cluster connectivity*, and $Inter\_Conn$ is the average of the maximum *inter-cluster connectivities* where averaging is over all clusters C_k. The intra-cluster connectivity of a cluster C_k is the proportion of connections between prototypes that reside inside C_k, to all connections that the prototypes of C_k have to any other prototypes. The inter-cluster connectivity of two clusters C_k, C_l is the proportion of connections between prototypes of C_k and C_l (in either direction), to all connections (to any cluster) of those prototypes in C_k which have at least one connection to C_l. Both $Intra\_Conn$ and $1 - Inter\_Conn$ are 1 when all clusters are completely separated. The value ranges of these measures are shown in

Table 1 Quality measures (explained in the text) for clusterings of the same (Subject 2) fMRI data from three different SOMs, with best in bold face and worst in italics

SOM size	Nr clusters	*DBI* $0 \leftarrow \infty$	*PBM* $0 \rightarrow \infty$	CD_{bw} $0 \rightarrow \infty$	*CONNind* $0 \rightarrow 1$	*Intra_Conn* $0 \rightarrow 1$	*Sep_Conn* $0 \rightarrow 1$
10×10	18	2.854	**0.0008**	*0.023*	*0.364*	*0.535*	*0.681*
20×20	25	*2.934*	0.0007	**0.027**	0.408	0.550	0.741
40×40	29	**2.761**	*0.0006*	0.025	**0.572**	0.**716**	**0.799**
60×60	—	—	—	—	—	—	—

Value ranges and arrows pointing from worst to best are under the respective measures

Table 1, along with arrows pointing from worst to best value. Sep_Conn stands for $1 - Inter\_Conn$. While it is hard to compare open-ended indexes, it is helpful to know that DBI values tend to be below 10, and $DBI > 1$ indicates overlaps but $DBI < 1$ does not necessarily mean separated clusters. CD_{bw} values can be much larger. PBM is scaled by $\frac{1}{K^2}$ where K is the number of clusters, which can make its values magnitudes smaller compared to DBI.

Quality measures for clusterings of the same fMRI data from SOMs of three different sizes are summarized in Table 1. Both DBI and CD_{bw} assign very similar scores to all SOMs although the 40×40 SOM is slightly better by the DBI and the 20×20 SOM by the CD_{bw}. However, given the typical value ranges of these indices all scores are poor, and the differences are negligible. A reasonable explanation is the model-dependence of these indices. DBI misjudges clusterings with non-spherical and unevenly sized clusters. CD_{bw} is likely failing because of possibly heterogeneous densities. If we ignored the quadratic penalty by PBM (scaled it back by K^2, i.e., 324, 625, and 841, respectively) it would indicate substantial differences, progressively to the advantage of the larger SOM. While the 40×40 SOM is confirmed by experts as the best, the DBI, $CDbw$, and PBM have difficulty correctly judging the highly irregular fMRI clusters. $CONNindex$, in contrast, handles irregular clusters and shows significant increase, given its range, in quality from 10×10 to 40×40 SOM size. Examining the components of $CONNindex$, the 40×40 SOM preforms significantly better in both metrics. It is noteworthy though that the larger increase is in the intra-cluster connectivity term, indicating more self-contained clusters. This is due to a sufficient number of prototypes for accurate mapping of the manifold structure, increasing the proportion of connections inside clusters regardless of their shapes. The connectivity measure senses this improvement correctly. No sensible cluster extraction could be done from a 60×60 SOM, which we attribute to the highly mixed an noisy signals (discussed below) in fMRI voxels. The 60×60 SOM has enough prototypes to begin to model the structure of the noise rather than the characteristics of the functional regions we aim to capture.

fMRI data is highly complex, partly because the voxels are large compared to the spatial extent of distinct neuronal signals and the variations of tissue types. This results in heavily mixed signals (time-courses) of tissue types and functional regions within a voxel. Exacerbating this mixing is the nature of the BOLD signal, which is

not always constant within the same functional region. It reflects overlapping spatial and temporal influences, potentially from many voxels depending on the functional region, subject and other factors. The result is a large degree of overall mixing that dilutes the discriminating characteristics of distinct functional regions. Figure 2d is an illustration of the level of similarity.

While formal optimization of SOM size is beyond the scope of this paper, we can also draw approximate justification for the 40×40 SOM from a Growing SOM (GSOM, [17]), which returns a $7 \times 6 \times 4 \times 4 \times 3 \times 2 \times 2$ SOM. With the last two dimensions close to vanishing the rest of this SOM comprises 2016 neurons, a number close to the 1600 neurons in the 40×40 SOM we use, and much larger than the number of neurons in a 10×10 or 20×20 SOM.

5 Results from Multiple Subjects

Figure 5 shows the localization of filtered clusters extracted from 40×40 SOMs and mapped back to the three-dimensional brains for each of the six subjects. The presented clusters belong to brain regions involved in the visual processing and motor response, and show commonality of the activated areas across subjects. Representative slices are chosen to exhibit the visual, motor, and supplementary motor cortex. Not all extracted clusters can be displayed in each of the three slices. For example in subject 2 the activation in the visual cortex is shown in the coronal slice, but not in the more laterally located sagittal slice. The visual cortex and cuneus (the group of green clusters in the coronal slices, and at the bottom of the sagittal slices) are activated by the visual stimulus. The left motor cortex and sensory cortex (red clusters at right in the axial, and at top in the sagittal slices) are active, consistent with squeezing the ball with right hand. Subjects 1, 2, and 6 exhibit some bi-lateral activity of the motor areas, with the larger response in the left brain (corresponding to the movement in the right hand). The supplementary motor area, also used in the generation of movement, is activated in each subject (red clusters at the center of the axial slices) with subjects 1 and 3 generating the largest and most coherent response areas. A number of clusters also appear, consistently across subjects, in other functional regions such as the superior and medial frontal gyri (magenta colors). While those, and several more that map to other brain slices (e.g., cerebellum, thalamus, cyngulate gyrus, precuneus, and caudate nucleus, not shown here) may correlate with the visual cortex to lesser extent, their common activation in all (or most) subjects calls attention to relationships worth investigating, and may hold keys to new discoveries of neuronal processes.

We note that, since clusters reflect similarity of time-courses, the same cluster may occur in multiple areas. For example, in the axial slice of subject 4, the green clusters cover parts of the sensory cortex (adjacent to the red motor cortex cluster at center right) and a section of the precuneus (the green cluster at the bottom of the slice). This means in subject 4 these areas are highly correlated, likely a result of

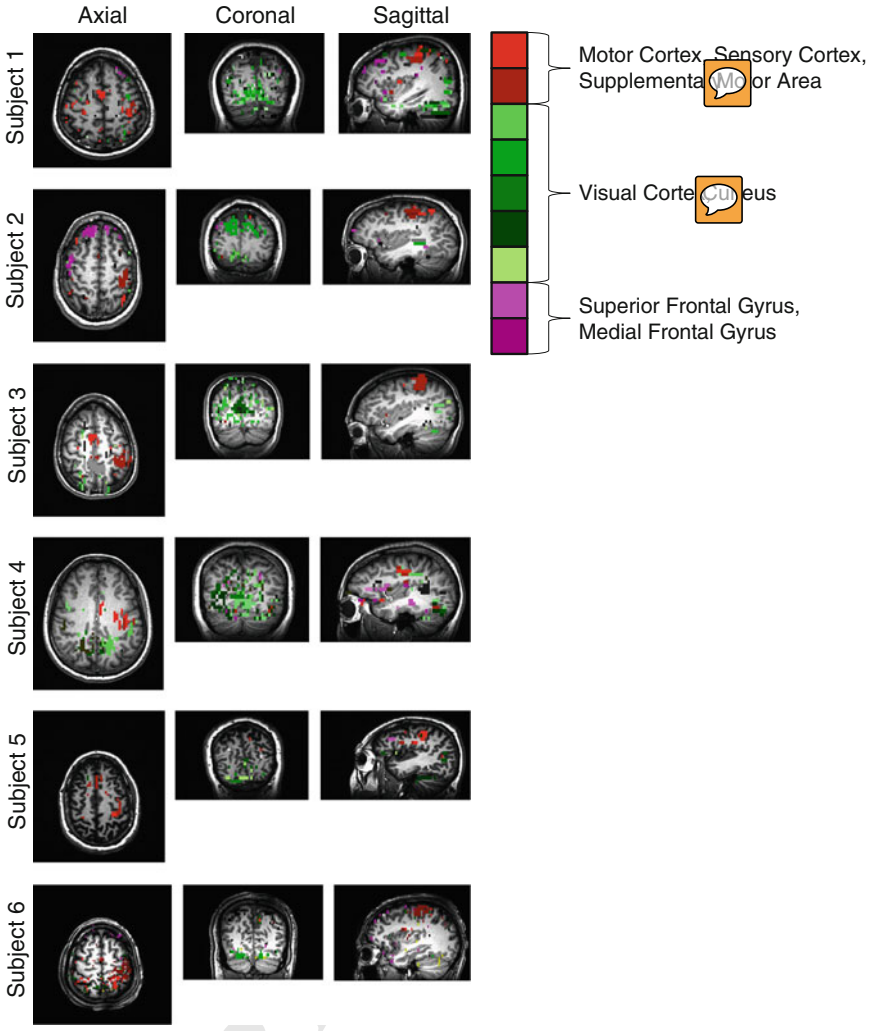

Fig. 5 Filtered clusters shown for all six subjects, in selected axial, coronal, and sagittal slices on the anatomical substrate. Here we only show clusters which occur in all subjects in the motor cortex, supplementary motor area and visual cortex (where activation is expected during our experiment), and in the cuneus, superior frontal gyrus, and medial frontal gyrus. The color wedge codes clusters which are present in these slices. Cluster colors are grouped into three hues that signify closely related functional/anatomical regions. The slices shown are selected to display the same functional regions in each subject. (Geometric co-registration remains a follow-up task at this time.)

a slightly different neural pathway that subject 4 uses to complete the task. Slight deviations of the pathways are expected in each subject. Thus, the same level of correlation between the same regions is not common in all subjects.

6 Conclusions

Our objective is to call attention to the untapped potentials of larger SOMs than those ($\sim 10 \times 10$) typically employed in fMRI analyses; to CSOM; and to connectivity (non-distance-based) measures, for better SOM manifold learning and cluster extraction. To that end we demonstrate, through real, full-brain fMRI data that increasing the SOM size up to a point (40×40 lattice in our case) facilitates cleaner capture of more relevant clusters than small SOMs. Importantly, further increase of the SOM size is detrimental to the clustering. We provide justification that this is due to the highly mixed and noisy time-course signals in fMRI data. Clusters in functional regions relevant to the generation of willed movement (the goal-oriented task we analyze), as well as others, are consistently identified from 40×40 SOMs across six subjects. This in turn supports more detailed elucidation of the functional relationships of brain regions and potentially allows discoveries of more nuanced neuronal activities related to the goal-oriented task. Follow-up work will strive for more comprehensive computational experiments and more formal investigation of the dependence of SOM sizes on the data characteristics.

References

1. Kohonen, T.: Self-Organizing Maps, 2nd edn. Springer, Berlin (1997)
2. Peltier, S.J., Polk, T.A., Noll, D.C.: Detecting low-frequency functional connectivity in fMRI using a Self-Organizing Map (SOM) algorithm. Hum. Brain Mapp. **20**, 220–226 (2003)
3. Wiggins, J.L., Peltier, S.J., Ashinoff, S., Weng, S.-J., Carrasco, M., Welsh, R.C., Lord, C., Monk, C.S.: Using a Self-Organizing Map algorithm to detect age-related changes in functional connectivity during rest in autism spectrum disorders. Brain Res **1380**, 187–197 (2011). Mar
4. Fischer, H., Hennig, J.: Neural network-based analysis of MR time series. Magn. Reson. Med. **41**(1), 124–131 (1999)
5. Erberich, S.G., Willmes, K., Thron, A., Oberschelp, W., Huang, H.: Knowledge-based approach for functional MRI analysis by SOM neural network using prior labels from talairach stereotaxic space. Med. Imag. pp. 363–373 (2002)
6. Hausfeld, L., Valente, G., Formisano, E.: Multiclass fMRI data decoding and visualization using supervised Self-Organizing Maps. NeuroImage **96**, 54–66 (2014)
7. ODriscoll, P.: Using Self-Organizing Maps to discover functional relationships of brain areas from fMRI images. Masters thesis, Rice University (2014)
8. Cox, R.W.: AFNI: Software for analysis and visualization of functional magnetic resonance neuroimages. Comput. Biomed. Res. **29**(0014), 162–173 (1996)
9. DeSieno, D. Adding a conscience to competitive learning. In: Proceeding of ICNN, July 1988 (New York) vol. I, pp. 117–124, (1988)
10. Merényi, E., Jain, A., Villmann, T.: Explicit magnification control of Self-Organizing Maps for "forbidden" data. IEEE Trans. Neural Netw. **18**, 786–797 (2007). May
11. Merényi, E.: Precision mining of high-dimensional patterns with Self-Organizing Maps: interpretation of hyperspectral images. In: Sinčak, P., Vasčak J. (eds.) Quo Vadis Computational Intelligence, Vol 54. Physica-Verlag, (2000)
12. Tasdemir, K., Merényi, E.: Exploiting data topology in visualization and clustering of Self-Organizing Maps. IEEE Trans. Neural Netw. **20**(4), 549–562 (2009)
13. Lötsch, J., Ultsch, A.: Exploiting the structures of the U-matrix. In: Advances in Self-Organizing Maps and Learning Vector Quantization, pp. 249–257. Springer (2014)

14. Ultsch, A., Siemon, H.P.: Kohonen's self organizing feature maps for exploratory data analysis. vol. 1, pp. 305–308 (1990)
15. Davies, D.L., Bouldin, D.W.: A cluster separation measure. IEEE Trans. Pattern Anal. Mach. Intell. **2**, 224–227 (1979)
16. Tasdemir, K., Merényi, E.: A validity index for prototype based clustering of data sets with complex structures. IEEE Trans. Syst. Man Cybern. Part B **41**, 1039–1053 (2011). August
17. Bauer, H.-U., Villmann, T.: Growing a hypercubical output space in a Self-Organizing Feature Map. IEEE Trans. Neural Netw. **8**(2), 218–226 (1997)

Author Queries

Chapter 22

Query Refs.	Details Required	Author's response
	No queries.	

Part V
Learning Vector Quantization Theories and Applications I

340050_1_En_5_PartFrontmatter ☑ TYPESET ☐ DISK ☐ LE ☑ CP Disp.:18/12/2015 Pages: 2 Layout: T1-Standard

Author Queries

Chapter 0

Query Refs.	Details Required	Author's response
	No queries.	